JCI insight

Task-related fMRI BOLD response to hyperinsulinemia in healthy older adults

Victoria J. Williams, … , David H. Salat, Steven E. Arnold

JCI Insight. 2019;4(14):e129700. https://doi.org/10.1172/jci.insight.129700.

Clinical Medicine | Aging | Endocrinology

There is growing evidence to suggest that the brain is an important target for insulin action and that states of insulin resistance may extend to the CNS, with detrimental effects on cognitive functioning. Although the effect of systemic insulin resistance on peripheral organs is well studied, the degree to which insulin affects brain function in vivo remains unclear.

This randomized, single-blinded, 2-way–crossover, sham-controlled, pilot study determined the effects of hyperinsulinemia on functional MRI (fMRI) brain activation during a 2-back working memory task in 9 healthy older adults (aged 57–79 years). Each participant underwent 2 clamp procedures (an insulin infusion and a saline placebo infusion, with normoglycemia maintained during both conditions) to examine the effects of hyperinsulinemia on task performance and associated blood oxygen level–dependent (BOLD) signal using fMRI.

Hyperinsulinemia (compared with saline control) was associated with an increase in both the spatial extent and relative strength of task-related BOLD signal during the 2-back task. Further, the degree of increased task-related activation in select brain regions correlated with greater systemic insulin sensitivity as well as decreased reaction times and performance accuracy between experimental conditions.

Together, these findings provide evidence of […]

JCI insight

CLINICAL MEDICINE

Task-related fMRI BOLD response to hyperinsulinemia in healthy older adults

Victoria J. Williams,[1,2] Bianca A. Trombetta,[1] Rabab Z. Jafri,[3,4] Aaron M. Koenig,[1,2] Chase D. Wennick,[1] Becky C. Carlyle,[1,2] Laya Ekhlaspour,[3,4] Rexford S. Ahima,[5] Steven J. Russell,[3,4] David H. Salat,[6,7] and Steven E. Arnold[1,2]

[1]Department of Neurology, Alzheimer's Clinical and Translational Research Unit, Massachusetts General Hospital, Boston, Massachusetts, USA. [2]Harvard Medical School, Boston, Massachusetts, USA. [3]Diabetes Research Center and Pediatric Endocrine Unit and [4]Diabetes Unit and Department of Medicine, Massachusetts General Hospital and Harvard Medical School, Boston, Massachusetts, USA. [5]Division of Endocrinology, Diabetes and Metabolism, Johns Hopkins School of Medicine, Baltimore, Maryland, USA. [6]Brain Aging and Dementia Laboratory, Athinoula A. Martinos Center for Biomedical Imaging, Department of Radiology, Massachusetts General Hospital, Boston, Massachusetts, USA. [7]Neuroimaging Research for Veterans Center, VA Boston Healthcare System, Boston, Massachusetts, USA

BACKGROUND. There is growing evidence to suggest that the brain is an important target for insulin action and that states of insulin resistance may extend to the CNS, with detrimental effects on cognitive functioning. Although the effect of systemic insulin resistance on peripheral organs is well studied, the degree to which insulin affects brain function in vivo remains unclear.

METHODS. This randomized, single-blinded, 2-way–crossover, sham-controlled, pilot study determined the effects of hyperinsulinemia on functional MRI (fMRI) brain activation during a 2-back working memory task in 9 healthy older adults (aged 57–79 years). Each participant underwent 2 clamp procedures (an insulin infusion and a saline placebo infusion, with normoglycemia maintained during both conditions) to examine the effects of hyperinsulinemia on task performance and associated blood oxygen level–dependent (BOLD) signal using fMRI.

RESULTS. Hyperinsulinemia (compared with saline control) was associated with an increase in both the spatial extent and relative strength of task-related BOLD signal during the 2-back task. Further, the degree of increased task-related activation in select brain regions correlated with greater systemic insulin sensitivity as well as decreased reaction times and performance accuracy between experimental conditions.

CONCLUSION. Together, these findings provide evidence of insulin action in the CNS among older adults during periods of sustained cognitive demand, with the greatest effects noted for individuals with highest systemic insulin sensitivity.

FUNDING. This work was funded by the NIH (5R21AG051958, 2016).

Conflict of interest: AMK has held full-time employment at Biogen and Sage Therapeutics, from which he earned a salary and received stock options. SJR has a patent and patents pending (US 9833570 B2) on aspects of the bionic pancreas; these patents are assigned to Massachusetts General Hospital and are licensed to Beta Bionics; has received honoraria and/or travel expenses for lectures from Dexcom, Eli Lilly, Tandem Diabetes, Sanofi, Novo Nordisk, Roche, and Ascensia; serves on the scientific advisory boards for Unomedical and Companion Medical; has served on a scientific advisory board for Tandem Diabetes; has received consulting fees from Senseonics and Flexion Therapeutics; has received grant support from Zealand Pharma, Novo Nordisk, and Beta Bionics; and has received in-kind support in the form of technical support and/or donation of materials from Eli Lilly, Zealand Pharma, Dexcom, Ascensia, Senseonics, Adocia, and Tandem Diabetes. SEA has received honoraria and/or travel expenses for lectures from AbbVie, Biogen, Merck, and Roche; has served on scientific advisory boards for Merck, Roche, T3D, and vTv; has received consulting fees from Cognito Therapeutics, M3 Biotechnology, Orthogonal Neuroscience, and Pain Therapeutics; and has received research grant support from AbbVie, Amylyx, EIP Pharma, and Merck.

Submitted: April 19, 2019
Accepted: June 13, 2019
Published: July 25, 2019.

Reference information: *JCI Insight*. 2019;4(14):e129700. https://doi.org/10.1172/jci.insight.129700.

Introduction

Nearly 30.3 million Americans have diabetes and another 84.1 million have prediabetes (1), representing a growing population in which insulin resistance is a major clinical concern. Even in nondiabetic adults, increasing insulin resistance is associated with accelerated cognitive decline (2, 3), cerebral atrophy (4, 5), and altered cerebral blood flow and metabolism (6, 7). Insulin signaling serves a neuromodulatory role within the CNS (8–12), and evidence of cerebral insulin resistance in both aging and Alzheimer's disease (AD; refs. 10, 13–18) has prompted investigations of insulin-mediated effects on brain function in vivo.

Experimentally increasing circulating insulin levels to stimulate insulin signaling in the CNS appears to benefit cognition (19–23), yet the effects of insulin on cerebral activity/metabolism across imaging modalities have been mixed (24–27) and may vary by peripheral insulin sensitivity (28, 29). Functional MRI (fMRI) studies manipulating insulin levels among young adults have reported *increased* fMRI-indexed activation during a memory task (30) yet *reduced* activation in response to a simple checkerboard pattern (26), with discrepant findings potentially relating to differences in cognitive demand between study tasks. Because

Table 1. Basic demographics of study sample

	Mean (SD)	Min	Max
Age (yr)	64.9 (7.7)	57	79
Education (yr)	16.7 (3.5)	9	20
MMSE	29.4 (0.7)	28	30
BMI (kg/m^2)	25.0 (5.2)	18.95	34.06
HEC-ISI	0.095 (0.041)	0.028	0.145
HOMA-IR	1.78 (1.71)	0.61	5.85
QUICKI	0.37 (0.04)	0.30	0.42
Fasting glucose (mmol/L)	94.2 (7.4)	85	107
Hemoglobin A1c (mmol/mol)	5.2 (0.2)	5	5.5
Time between sessions (d)	19.4 (18.5)	7	63

n = 9 (8 males and 1 female). MMSE, Mini-Mental Status Examination; HEC-ISI, Hyperinsulinemic Normoglycemic Clamp–Insulin Sensitivity Index; HOMA-IR, Homeostatic Model Assessment of Insulin Resistance; QUICKI, Quantitative Insulin Sensitivity Check Index.

insulin-dependent glucose uptake by the CNS is observed only during periods of sustained cognitive effort (31), insulin-mediated effects may be less readily observed during more passive tasks.

Here, we implemented a hyperinsulinemic normoglycemic clamp procedure (32) to investigate repeated-measure fMRI signal change between insulin and saline conditions during a sustained working memory task among older adults. We expected to observe greater fMRI activity during insulin infusion compared with saline infusion, the degree to which would additionally correlate with insulin sensitivity and task performance.

Results

Participant characteristics

From an initial recruitment of 17 participants, 4 failed screening or declined to participate, 3 had incomplete fMRI data (because of scanner malfunction or difficulty establishing reliable i.v. lines to administer the infusion), and 10 passed screening and completed the 2 experimental visits between February 2017 and April 2018. Of the 10 participants who completed, 1 participant was excluded from all fMRI analyses because of excessive motion artifacts during scan acquisition. Demographic information for the final sample of 9 participants is reported in Table 1 and consisted of 8 males and 1 female ranging in age from 57 to 79 years, with a mean age of 65 years (SD = 6.88) and a mean education level of 16 years (SD = 3.46). All participants scored above a level associated with cognitive impairment on the Mini-Mental Status Examination (MMSE) (mean 29.44, SD 0.73, range 28–30). The order of insulin versus saline visits was balanced across all participants (4 saline-insulin, 5 insulin-saline). The average time span between the 2 experimental visits for the majority of participants (8 of 9) was 2 weeks (mean = 14.0 days; SD = 9.2 days), with 1 outlying participant measuring 63 days between experimental visits.

Assessment of insulin sensitivity

Insulin sensitivity was assessed using 3 methods: blood-based measures (screening visit hemoglobin A1c and fasting glucose levels) used to calculate the Quantitative Insulin Sensitivity Check Index (QUICKI) and Homeostatic Model Assessment of Insulin Resistance (HOMA-IR) scores averaged across both experimental visits and the Hyperinsulinemic Normoglycemic Clamp–Insulin Sensitivity Index (HEC-ISI) score derived from the insulin clamp procedure, serving as the gold standard metric of insulin sensitivity (Table 1). Baseline blood-based calculated insulin sensitivity metrics were significantly correlated between the 2 experimental visits (QUICKI: $\rho = 0.886$, $P = 0.001$; HOMA-IR: $\rho = 0.937$, $P < 0.001$) and were averaged to yield a single QUICKI and HOMA-IR score for each participant. As expected, the average QUICKI and HOMA-IR scores were significantly correlated with the experimentally derived HEC-ISI score ($\rho = 0.753$, $P = 0.019$; and $\rho = -0.771$, $P < 0.015$, respectively). Age was not significantly associated with HEC-ISI, QUICKI, or HOMA-IR scores ($\rho = -0.035$, $\rho = 0.079$, $\rho = -0.054$, respectively; all $P > 0.05$). All participants demonstrated insulin sensitivity levels below clinical cutoffs for diabetes, but 1 participant met criteria for insulin resistance.

Table 2. Glucose/insulin levels during clamp

	Saline mean (SD)	Insulin mean (SD)
At clamp baseline		
Serum insulin (mU/L)	6.8 (7.6)	8.5 (7.1)
Blood glucose (mmol/L)	5.3 (0.5)	5.2 (0.6)
Across steady-state period		
Serum insulin (mU/L)[A]	5.1 (4.5)	114.8 (38.7)
Blood glucose (mmol/L)	92.2 (5.4)	92.3 (8.3)
Blood glucose variability[A]	6.1 (3.0)	12.3 (4.8)
Percentage of time glucose within range (80–140 mmol/L)[B]	94.8 (6.7)	85.5 (9.1)
Dextrose i.v. rate (mL/hr)[A]	0 (0)	275.6 (95.4)

Significant difference between saline and insulin conditions based on 2-tailed, paired-sample *t* test ($n = 9$): [A]$P < 0.01$; [B]$P < 0.05$.

Blood insulin and glucose levels were measured at clamp baseline, as well as averaged across all time points within the steady-state period, reported in Table 2. Using a 2-tailed, paired-sample *t* test, blood glucose levels were not significantly different at baseline between the insulin and saline conditions ($t[8] = -1.53$; $P > 0.05$). During steady state, mean serum insulin concentration across all participants was 114.8 (38.7 SD) mU/L during the hyperinsulinemic normoglycemic clamp procedure and 5.1 (4.5 SD) mU/L during the saline clamp procedure, yielding a 28-fold increase in serum insulin concentration during the insulin infusion. Paired-sample *t* tests demonstrated that average blood glucose levels did not differ during the steady-state period between conditions ($t[8] = 0.04$; $P > 0.05$), although glucose levels were maintained within the target range (80–140 mmol/L) more consistently during the saline compared with insulin infusion ($t[8] = 3.03$; $P = 0.02$).

Behavioral fMRI task results

Behavioral task data are presented in Table 3. At the group level, there were no significant differences between insulin and saline conditions in mean accuracy or mean reaction time for either 0-back or 2-back trials when analyzed using paired-sample *t* tests ($P > 0.05$). Individual difference scores in task accuracy and reaction time between experimental conditions were calculated and served as covariates of interest in subsequent analyses (*Association between BOLD signal change and N-back task performance*).

fMRI analyses

Task-related activation during insulin and saline conditions. Figure 1A shows the independent and overlapping effects of mean blood oxygen level–dependent (BOLD) signal during the 2-back to 0-back contrast for each experimental condition (insulin and saline) analyzed separately. An expected pattern of fMRI BOLD signal activation was observed for *both* experimental conditions during the 2-back task within bilateral superior parietal, dorsolateral prefrontal, superior and medial frontal, insular, and superior cerebellar cortices, as well as bilateral clusters in the thalamus and caudate ($P < 0.01$ and corrected for multiple comparisons).

Table 3. Behavioral results for N-back task

	Saline mean (SD)	Insulin mean (SD)
0-Back reaction time (seconds)	0.593 (0.060)	0.594 (0.049)
2-Back reaction time (seconds)	0.753 (0.056)	0.774 (0.056)
0-Back accuracy (%)	99.15 (1.81)	98.58 (2.60)
2-Back accuracy (%)	94.59 (4.87)	95.58 (2.60)

Two-tailed, paired-sample *t* tests ($n = 9$) revealed no significant differences between saline and insulin conditions (all $P > 0.05$).

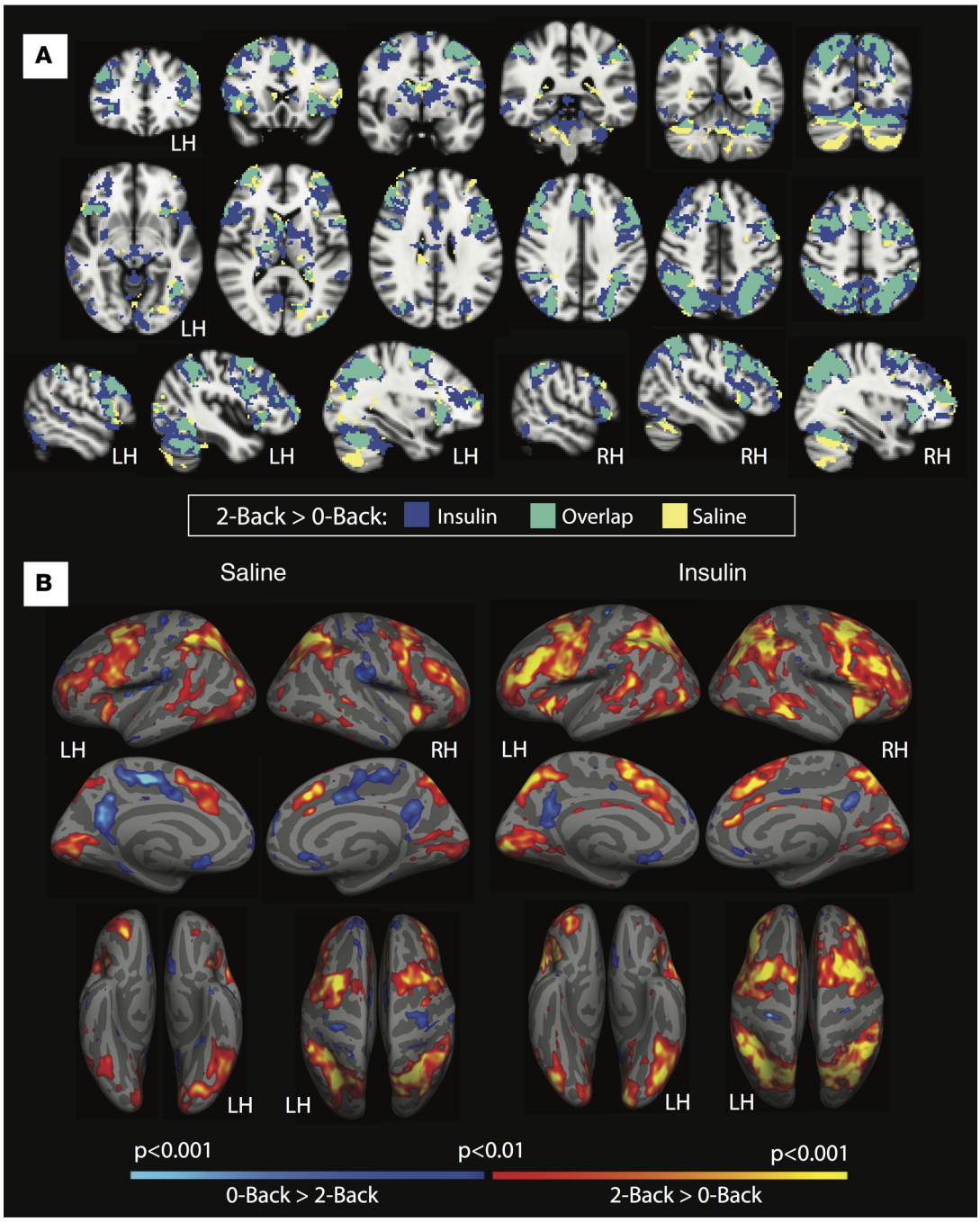

Figure 1. Spatial overlap of task-related fMRI activation for 2-back greater than 0-back trials during insulin and saline conditions analyzed separately. (**A**) Conjunction map showing the spatial overlap from 1-sample group mean analyses of task-related activation for 2-back to 0-back trials for insulin and saline conditions analyzed separately (n = 9; P < 0.01, corrected). An expected pattern of task-related activation was observed across both conditions largely involving frontal and parietal regions, although the spatial extent of activation was 1.8 times larger during insulin compared with saline condition. (**B**) Results from each 2-back to 0-back contrast analyzed separately by experimental condition (insulin and saline) contributing to the conjunction map above, resampled onto the cortical surface for ease of viewing.

However, the spatial extent of task-related BOLD activation during the insulin clamp procedure was 1.8 times greater than during the saline condition (insulin only = 204,464 mm^3; saline only = 57,112 mm^3; overlap = 127,800 mm^3). Resultant significance maps for each condition analyzed separately were projected onto the cortical surface for visualization (Figure 1B).

Complementing the conjunction map in Figure 1A, additional higher-level analyses directly compared the degree of activation between the 2 conditions. Figure 2A demonstrates the results of a higher-level anal-

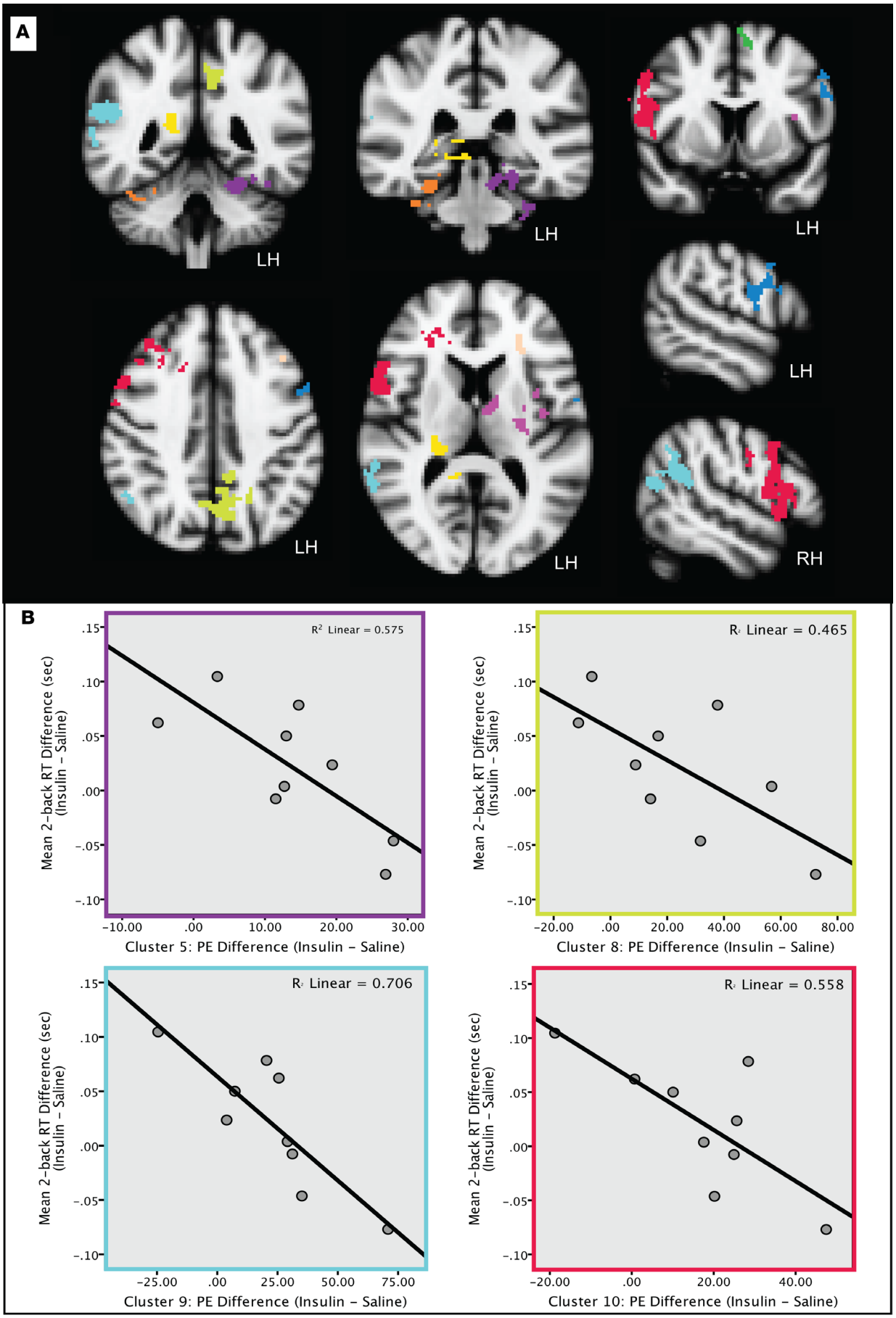
A
LH
LH
LH
LH
LH
LH
RH
B
R² Linear = 0.575
Mean 2-back RT Difference (sec) (Insulin – Saline)
Cluster 5: PE Difference (Insulin – Saline)
R² Linear = 0.465
Cluster 8: PE Difference (Insulin – Saline)
R² Linear = 0.706
Cluster 9: PE Difference (Insulin – Saline)
R² Linear = 0.558
Cluster 10: PE Difference (Insulin – Saline)

Figure 2. Brain areas showing significantly increased task-related fMRI activation during insulin compared to saline conditions, and regional associations with task performance and baseline insulin sensitivity. (**A**) Cluster-based results of a 2-step higher-level analysis to evaluate average within-subject difference in 2-back to 0-back contrast between insulin and saline conditions (n = 9). First, subject-level repeated-measure analysis was performed to yield a single cope comparing blood oxygen level–dependent (BOLD) signal during the contrast of interest (2-back to 0-back) between insulin and saline runs. Next, each within-subject difference cope was entered into a single 1-sample group mean regression model to identify brain regions that consistently demonstrated a change in BOLD signal during the 2-back task between the insulin and saline conditions, such that the mean change in activation across all participants was significantly different from the null hypothesis of no change. Final Z-statistic maps were thresholded using clusters determined by $Z > 2.3$ ($P < 0.01$) and a corrected cluster significance threshold of $P < 0.05$. Significant differences in task-related BOLD signal were noted in bilateral inferior frontal, parahippocampal, precuneus, and thalamic regions, as well as lateralized clusters within right superior frontal, right supramarginal, and left middle frontal cortices. (**B**) Scatter plots demonstrating significant bivariate correlations between the degree of BOLD signal parameter estimate (PE) change during insulin compared with saline conditions and difference in RT on 2-back trials between conditions (n = 9; $P < 0.05$ for all). Colored outline around scatter plots corresponds to the matching cluster color from which its data were extracted. Clusters are described in greater detail in Table 4 (cluster 5, left fusiform/supramarginal gyrus; cluster 8, bilateral precuneus; cluster 9, right supramarginal/angular gyrus; and cluster 10, right inferior frontal cortex).

ysis averaging the degree of within-subject BOLD signal change between insulin and saline conditions of all participants. As reported in Table 4, a total of 10 clusters remained after thresholding at $P < 0.01$ and correcting for multiple comparisons. Brain regions in which task-related BOLD signal during insulin was significantly greater than BOLD signal during saline largely coincided with brain areas identified during the within-subject analysis (reported above), including bilateral middle and superior frontal cortices, insular cortex, caudate, and thalamus. Additional areas that emerged as showing significantly greater activation during insulin compared with saline included bilateral middle temporal and precuneus regions and left parahippocampal cortex. For each cluster, the average parameter estimates (PEs) of the effect of insulin compared with saline during the 2-back to 0-back contrast were extracted from each participant's within-subject midlevel analysis and imported into SPSS for further investigation. No statistically significant findings were identified for the opposite contrast of saline greater than insulin. Age and BMI were not significantly correlated with mean task-related activation (2-back to 0-back) for either insulin or saline conditions or with the difference in task-related fMRI activation between experimental conditions (all correlation coefficients $P > 0.05$).

Association between BOLD signal change and systemic insulin sensitivity. As described in *Task-related activation during insulin and saline conditions*, significant clusters demonstrating greater task-related activation during insulin compared with saline conditions across subjects were used as regions of interest (ROIs) for subsequent statistical analyses. For each ROI, PEs were extracted from the within-subject analysis of mean task-related activation (2-back to 0-back) for each experimental condition analyzed separately (insulin and saline) as reported in Table 4. PEs from the saline condition were subtracted from the insulin condition PEs to compute a difference score for each ROI. To determine whether the degree of increased activation during insulin compared with saline was associated with systemic insulin sensitivity, Pearson product moment correlation coefficients were computed for each cluster. Of the 10 clusters, HEC-ISI was significantly associated with the degree of task-related BOLD signal increase during the insulin condition in the bilateral precuneus (cluster 8: $\rho = 0.743$, $P = 0.022$), such that those individuals with greater insulin sensitivity showed the greatest increase in task-related activation during the insulin compared with saline condition (shown in Figure 3). The association between HEC-ISI and change in BOLD signal between conditions in cluster 8 remained significant even after controlling for age in a partial correlation model ($\rho = 0.748$, $P = 0.033$).

Association between BOLD signal change and N-back task performance. The same ROI clusters defined in *Task-related activation during insulin and saline conditions* were also used to assess whether the degree of BOLD signal change between experimental conditions was associated with a change in task performance. As shown in Table 5 and Figure 2B, an increase in BOLD signal during the insulin compared with saline clamp was significantly associated with faster 2-back RTs on insulin days within 5 of the 10 clusters: LH fusiform/parahippocampal gyrus (cluster 5: $\rho = -0.758$, $P = 0.018$), RH thalamus/posterior cingulate (cluster 6: $\rho = -0.685$, $P = 0.042$), bilateral precuneus (cluster 8: $\rho = -0.682$, $P = 0.043$), RH supramarginal/angular gyrus (cluster 9: $\rho = -0.840$, $P = 0.005$), and RH inferior frontal/precentral gyrus (cluster 10: $\rho = -0.747$, $P = 0.021$). However, faster speed may come at the cost of accuracy given that a greater BOLD signal change between insulin and saline conditions within the RH paracingulate/superior frontal gyrus was associated with *reduced* accuracy on 2-back trials (cluster 2: $\rho = -0.740$, $P = 0.023$). Despite independent regional associations between behavioral performance and BOLD signal change between conditions, 2-back RT and accuracy difference scores were not significantly correlated with one another across participants ($\rho = 0.460$, $P > 0.05$).

Table 4. Significant clusters showing increased BOLD signal during 2-back task on insulin compared with saline

		Peak activation difference (MNI152 2 mm)				
	Volume (mm²)	X	Y	Z	Hemi	Anatomical description
Cluster 1	2104	28	−36	−24	RH	Fusiform, parahippocampal gyrus
Cluster 2	2376	12	26	46	RH	Paracingulate, superior frontal gyrus
Cluster 3	2392	−58	4	28	LH	Inferior frontal, precentral gyrus
Cluster 4	2432	−28	−6	12	LH	Putamen, thalamus
Cluster 5	2656	−24	−46	−18	LH	Fusiform, parahippocampal gyrus
Cluster 6	2672	24	−26	10	RH	Thalamus, posterior cingulate
Cluster 7	2736	−28	32	0	LH	Middle frontal gyrus
Cluster 8	3712	−4	−52	40	LH/RH	Precuneus
Cluster 9	4672	60	−44	22	RH	Supramarginal, angular gyrus
Cluster 10	10,160	62	12	16	RH	Inferior frontal, precentral gyrus

MNI152, Montreal Neurological Institute 152 atlas; RH, right hemisphere; LH, left hemisphere.

Discussion

In this pilot study of healthy, nondiabetic older adults, we show that an experimentally induced state of hyperinsulinemia (while maintaining normoglycemia) is associated with an increase in both the spatial extent and relative strength of BOLD signal during a concurrent working memory task. We additionally demonstrate that the degree of increased task-related activation in select brain regions correlates with both systemic insulin sensitivity as well as decreased RTs in the hyperinsulinemic versus control condition. Together, these findings support a beneficial action of insulin in the CNS among older adults during periods of sustained cognitive demand, with the greatest effects noted for individuals with the highest peripheral insulin sensitivity.

To date, only a small number of studies have used an insulin clamp technique to assess brain-specific effects of increasing circulating insulin. Electroencephalography (EEG) studies have shown that increasing insulin has no effect on visual evoked potentials (24, 26), although when measured concurrently with an auditory memory task, insulin infusion is associated with reduced P300 amplitude within parietal regions (24). An early pioneering study using magnetoencephalography showed that both spontaneous and task-related cortical activity was increased with insulin infusion in healthy, lean adults, though this finding did not extend to obese individuals (27). Positron emission tomography studies have demonstrated insulin-associated increases in cerebral glucose metabolism among subjects with impaired glucose tolerance (28, 29) but no evidence of insulin-induced changes in healthy younger adult samples (25). In fMRI studies among healthy younger adults, insulin infusion is associated with *increased* task-related fMRI activation during a novel picture-encoding task along with improved RTs (30). However, a second study of similarly healthy adults observed *reduced* BOLD signal in response to a simple visual stimuli (reversing checkerboard pattern) during hyperinsulinemia compared with when insulin levels were suppressed below basal levels (26). In the present study, we extend findings of insulin-associated effects on task-related fMRI activation to healthy older adults, where the magnitude of increased BOLD signal between insulin and saline conditions correlated with both behavioral performance and peripheral insulin sensitivity.

Given such heterogeneous findings across prior studies, key methodological differences may account for some of the observed discrepancies. Principally, it appears that an increased neural response to elevated circulating insulin occurs most readily when measured concurrently with a challenging cognitive task. The bulk of glucose uptake in the neurons is insulin independent, occurring primarily via GLUT1 and GLUT3 transporters (33), which serve to support neuronal energy metabolism (34) and facilitate glucose uptake into neurons from interstitial pools (35). Both of these mechanisms are easily saturated at low glucose concentrations, making their modulatory effects somewhat limited (36). On the other hand, GLUT4 transporters are often coexpressed with GLUT3 throughout the cerebral cortex and are entirely dependent on insulin signaling (16), thus providing a direct mechanism for insulin to promote additional glucose uptake during periods of sustained cognitive demand (31). Accordingly, diminished glucose uptake in the CNS is observed when circulating insulin is reduced below basal levels (37), and suppression of insulin signaling using a lipid infusion protocol results in

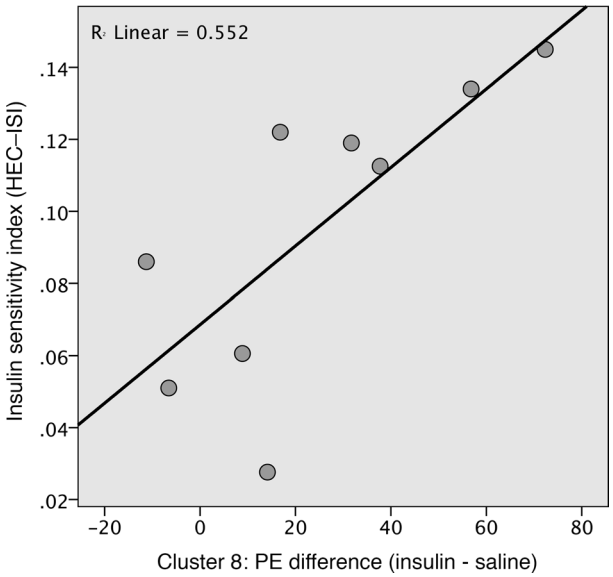

Figure 3. Scatter plot demonstrating a significant positive bivariate correlation between increased task-related activation during the insulin compared with saline clamp, quantified as a change in BOLD signal PE and hyperinsulinemic euglycemic clamp–insulin sensitivity index (HEC-ISI) within the bilateral precuneus (cluster 8); n = 9.

reduced cellular energy production in relation to concurrent energy expenditure during periods of sustained cognitive activity (38). It is therefore plausible that investigating brain-specific effects of elevated insulin levels may be best tested under metabolically demanding conditions.

Behaviorally, we observed improved RTs on 2-back trials associated with the degree of task-related BOLD increase between insulin and saline conditions within several clusters, including the RH thalamus, posterior cingulate, supramarginal gyrus, angular gyrus, and inferior frontal cortex; left parahippocampal regions; and bilateral precuneus. Previous epidemiological studies where circulating insulin levels were experimentally manipulated (through either insulin infusion or intranasal inhalation) have also demonstrated associations between cognitive functioning and induced hyperinsulinemia, where the effects of insulin seem to particularly benefit memory processes (19–22) although not in all cases (39). Randomized controlled clinical trials of regularly administered intranasal insulin treatment to patients with AD and mild cognitive impairment demonstrated longitudinal gains in memory performance, preserved brain volume, and a reduction in the tau-P181/AB42 ratio among those assigned to insulin compared with placebo (40, 41).

Finally, within-subject changes in BOLD signal between conditions were regionally associated with peripheral insulin sensitivity (HEC-ISI), such that participants with the highest insulin sensitivity showed the greatest increase in BOLD signal within the bilateral precuneus. Additional regions, including the right inferior frontal, lateral parietal, posterior cingulate, and left parahippocampal regions, also demonstrated a strong positive correlation between BOLD signal change and insulin sensitivity. Although these ROIs did not reach a level of statistical significance, the magnitude of the correlations was of moderate strength (all correlation coefficients >0.5), despite being underpowered by the limited sample size. Interestingly, intranasal insulin administration has been shown to attenuate progression of hypometabolism within the precuneus in those with mild cognitive impairment and mild or moderate AD compared with a placebo control group (41), supporting a beneficial effect of insulin action within brain regions most susceptible to AD pathology. In other studies of adults without dementia, baseline insulin resistance was shown to mediate insulin-induced increases in functional connectivity between prefrontal regions and the hypothalamus but only among individuals with the highest insulin sensitivity (42). In obese individuals, insulin sensitivity was also found to mediate the association between BMI and task-related fMRI activation in the right parietal lobe (43), and negative correlations between insulin sensitivity index and default mode network connectivity strength have also been demonstrated, independent of BMI (44). Differences in neuronal metabolism as a function of insulin sensitivity have also been reported (28, 29). Taken together, our work adds to a growing body of literature supporting the notion that impaired insulin signaling in the periphery likely extends to the brain. Targeted interventions aimed to enhance insulin sensitivity among older adults may be a useful clinical strategy to improve cognition.

Table 5. BOLD signal PEs and associations with insulin sensitivity and task performance

	BOLD signal PEs			Pearson's correlation coefficients		
	Saline (mean)	Insulin (mean)	PE difference score (insulin – saline)	HEC-ISI	RT difference	Accuracy difference
Cluster 1	3.88	14.72	10.84	0.126	0.060	0.376
Cluster 2	19.76	36.92	17.15	0.039	−0.417	**−0.740**[A]
Cluster 3	14.14	38.61	24.47	0.210	−0.343	−0.462
Cluster 4	4.10	14.39	10.29	0.406	−0.026	−0.251
Cluster 5	0.96	14.81	13.85	0.450	**−0.758**[A]	−0.482
Cluster 6	−3.23	10.63	13.86	0.513	**−0.685**[A]	−0.342
Cluster 7	10.36	26.39	16.03	0.502	−0.412	−0.562
Cluster 8	−2.14	22.37	24.51	**0.743**[A]	**−0.682**[A]	−0.460
Cluster 9	18.70	40.80	22.10	0.544	**−0.840**[B]	−0.356
Cluster 10	32.62	49.99	17.37	0.413	**−0.747**[A]	−0.507

One-sample group mean (n = 9) of BOLD signal PEs from linear regression models of 2-back to 0-back trials during insulin and saline conditions for each cluster, as well as the mean difference in PE between conditions. Pearson product moment correlations between PE difference score and HEC-ISI, 2-back trial reaction time (RT) difference between conditions, and 2-back trial accuracy difference between conditions. [A]$P < 0.05$. [B]$P < 0.01$. Bold values are significant.

Limitations. Despite the small sample size of this pilot study, we observed robust increases in task-related fMRI activation during hyperinsulinemia compared with a saline control condition with results thresholded at $P < 0.01$ and corrected for multiple comparisons. Because our sample was predominantly older adult males, we were unable to assess whether the cerebral response to hyperinsulinemia varied by sex or extended to a more expansive age range, and future studies should address these important limitations. Although regional task-related activation was associated with baseline insulin sensitivity in nondiabetic participants, further investigation comparing larger groups of nondiabetic, prediabetic, and diabetic individuals is warranted to clarify the pathophysiological roles of CNS and peripheral insulin signaling in regard to cognitive function. Further work should also address the role of other circulating hormones that vary in response to the clamp procedure that could also affect cerebral metabolism. Finally, several confounds are inherent to the clamp procedure that may have influenced our results, including fluctuating glucose levels during the insulin infusion as well as perturbations in glucose levels likely occurring during the transfer between the gurney and MRI scanner bed. However, glucose variability was not associated with BOLD signal during the insulin condition, and special care was taken to limit physical exertion throughout the clamp procedure.

Conclusions. In this pilot study, we showed that a state of hyperinsulinemia significantly increased task-related BOLD signal during a period of high cognitive demand among healthy older adults. We further demonstrated that the degree of signal change between clamp conditions correlated with both task performance and individual metrics of insulin sensitivity, suggesting a beneficial action of insulin in the CNS for both brain activation as well as cognitive performance.

Methods

Participants

Healthy older adults aged 55–85, fluent in English, deemed medically safe to undergo MRI procedures, with at least 12 years of formal education, were recruited to participate in a randomized, single-blinded, 2-way–crossover, placebo-controlled, pilot study to assess the effects of insulin on task-related fMRI brain activation during a cognitively demanding working memory task. Participants were recruited to the study in response to advertisement fliers posted on bulletin boards around Massachusetts General Hospital, as well as through an online posting in the Research Study Volunteer Program, RSVP for Health, registry for clinical research studies. All participants were cognitively intact (MMSE ≥ 26), with exclusion criteria consisting of any CNS disease or neurocognitive disorder; diabetes (or HbA1c ≥6.5 and fasting glucose >125 at screening); clinical laboratory blood work abnormalities (anemia, B_{12}, thyroid function, RPR); known hypersensitivity or allergy to latex; history of major psychiatric illness or alcohol/substance abuse

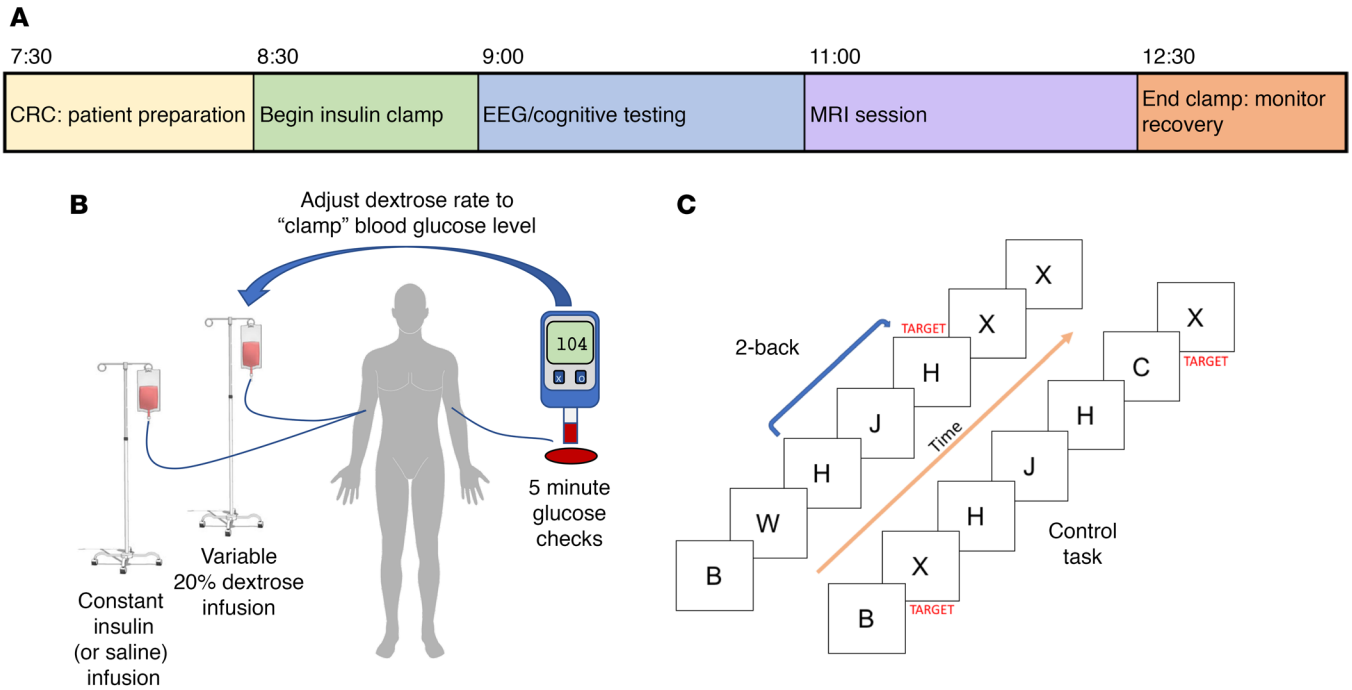

Figure 4. Overview of study procedures. (**A**) Overview of study timeline for each experimental visit (insulin and saline clamp conditions) conducted within the Massachusetts General Hospital, Clinical Research Center (CRC). Each infusion condition was implemented following an overnight 12-hour fast. Study tasks (consisting of electroencephalography [EEG], cognitive testing, and functional MRI [fMRI]) commenced as soon as steady state was achieved. (**B**) Schematic of clamp setup. A continuous infusion of either insulin or saline was administered alongside a variable dextrose infusion to maintain normoglycemia, as indicated by 5-minute-interval blood glucose level checks. (**C**) Overview of N-back working memory task that was given during each fMRI session concurrently with infusion procedure. For the 2-back trials, participants were required to respond by button press if the letter presented was exactly the same as 2 stimuli before. For the 0-back control trials, participants were instructed to press a response button immediately upon seeing the letter *X*.

within the previous 2 years, contraindications to the MRI environment (implanted metal, aneurysm clips, etc.); clinical history of pancreatic, liver or kidney disease; or current use of medications with psychoactive properties or anticoagulant therapy.

Hyperinsulinemic normoglycemic clamp procedure

Participants fasted for 12 hours before each of two 5-hour experimental visits (1 with insulin and the other saline placebo) spaced approximately 2 weeks apart. Participants were single blinded to experimental condition, and the order of clamp condition was systematically balanced across participants upon enrollment into the study. During the clamp procedure, cognitive testing, EEG, and structural/functional MRI data were collected once steady state was achieved as defined below (for an overview of study design, see Figure 4). Each clamp procedure was run by an experienced endocrinologist and a registered nurse within the CRC of the Massachusetts General Hospital research campus located in Charlestown, Massachusetts. Participants were situated on an MRI-compatible gurney for the duration of the experiment, except for a brief transfer onto the MRI console table during the scans. To begin the clamp procedure, i.v. cannulas were inserted into the antecubital vein of each arm, 1 for insulin infusion (or saline) and glucose, and the other for continuous blood sampling. The arm with the i.v. used for venous sampling was placed in a warming box for the duration of the clamp procedure, unless both hands were needed for cognitive testing and during the MRI scan. For the insulin condition, insulin infusate was prepared by adding regular insulin (Humulin R, Eli Lilly, 100 U/mL) to a solution of 2% human serum albumin in normal saline.

For the insulin clamp procedure, at time 0 a priming dose of 200 mU/m^2/min of insulin was given for 2 minutes, while concurrently starting a continuous infusion of 80 mU/m^2/min of insulin (roughly equal to 4–5 U/hr of insulin for an average-sized person). For the duration of the clamp, a small sample (≤0.5 cc) of venous blood was drawn every 5 minutes for real-time assessment of glucose levels using triplicate StatStrip glucose meters. Larger volume blood samples (5 cc) were drawn every 30 minutes throughout the pro-

cedure to assess serum insulin concentrations after the study. Five minutes after the initial insulin infusion, a variable 20% dextrose infusion was started to achieve normoglycemia (defined by a target glucose level of 90 mg/dL with an acceptable range of 80–140 mg/dL), with careful adjustment by the endocrinologist based on feedback from the real-time blood glucose levels. Steady-state normoglycemia (i.e., the glucose infusion rate equals glucose uptake by all tissues in the body) was considered to be achieved after the first 15-minute continuous segment in which a steady D20% glucose infusion rate was given and the glucose was maintained at 90 ± 10 mg/dL. Once steady state was achieved, study tasks commenced.

For the saline clamp procedure, all experimental procedures were identical to the insulin clamp described above, with the exception that a solution of 2% human serum albumin in normal saline infused at a rate of 100 cc/hr was substituted for insulin infusate, and 20% dextrose was administered as needed to maintain normoglycemic blood glucose levels within the target range of 80–140 mg/dL throughout the saline clamp procedure.

For the MRI session, all the infusion pumps were situated in the MRI console room, and participants were wheeled into the scanner bay on an MRI-compatible gurney and transferred to the scanner table. The i.v. infusion line was briefly disconnected from the pump to be run through the wave guide and reattached. The nurse accompanied the participant in the scanner room for the duration of the MRI session, and real-time blood draws were maintained throughout the scans by passing each blood sample through the wave guide.

Blood processing and insulin sensitivity metrics

Several indices of insulin sensitivity were collected for each participant. To assess study eligibility during the screening visit, fasting blood was drawn and baseline hemoglobin A1c and fasting glucose levels were obtained. Fasting blood was also collected at the beginning of each experimental visit, and HOMA-IR and QUICKI scores were calculated based on previously published formulas, with the following clinical cutoffs defining insulin resistance: HOMA-IR >2.5; QUICKI <0.339 (45).

Finally, as a gold standard measure of insulin sensitivity, the HEC-ISI score was calculated from data collected in the hour immediately following arrival at steady state. Serum concentrations of insulin were determined using an Iso-Insulin ELISA (Mercodia, 10-1128-01). Kits were purchased in bulk to avoid lot-to-lot variability and to maximize technical comparability of all measures. Assays were performed according to the manufacturer's instructions and published dilution recommendations. Serum samples and standard curves were run in duplicate on each plate. In addition, commercial insulin controls were included on each plate to monitor plate-to-plate consistency. Numerical data were fitted to a 4PL curve using Prism 7 (GraphPad) software to generate calculated concentrations. HEC-ISI was calculated as the ratio of the increment in glucose uptake (ΔR_d) to the increment in serum insulin concentration (ΔI), normalized to the ambient blood glucose concentration (G) at which the clamp was performed. HEC-ISI is defined as the glucose infused per lean body mass per time using the following formula: HEC-ISI = $\Delta R_d/(\Delta I \times G)$.

Behavioral N-back working memory task

Figure 4 depicts the study procedure timeline. Tasks began as soon as steady-state normoglycemia was achieved as described in "Hyperinsulinemic normoglycemic clamp procedure," with all tasks conducted simultaneously with the clamp procedure, allowing for investigation of the real-time effects of insulin on cognition and brain activity.

For the N-back working memory task, participants were provided task instructions and a trial run of the task before completing 2 experimental runs within the MRI scanner. For the 2-back condition, participants were instructed to press a button if the letter stimulus presented on the screen matched the letter stimulus that was presented 2 slides ago. A 0-back control condition was also performed in which participants were instructed to press a button each time the letter *X* appeared on the screen amid a stream of distractor letters. Each fMRI run consisted of 10 alternating blocks of 0-back and 2-back conditions (14 stimuli per block), for a total run time of 5 minutes and 12 seconds. Each individual's between-session difference in behavioral task performance (RT and accuracy), as well as BOLD signal change during the 2-back compared with 0-back contrast, served as the primary outcome metrics for subsequent data processing and analyses.

MRI acquisition and preprocessing

MRI data were collected on a research-dedicated 3T Siemens Prisma scanner equipped with a 64-channel head coil located at the Martinos Center for Biomedical Imaging. To serve as a registration template for functional scans, a single high-resolution, T1-weighted, multiecho magnetization-prepared rapid gradi-

ent-echo sequence was acquired in the sagittal plane with the following acquisition parameters: voxel size = 1 mm isotropic; matrix = 256 × 256; FOV = 256 mm; 176 sagittal slices; phase encoding anterior-posterior; flip angle = 7°; TR = 1870 ms; TE(s) = 1.69, 3.55, 5.41, and 7.27 ms; TI = 1000 ms; bandwidth = 650 Hz/pixel; nonselective inversion recovery; and acquisition time 2 minutes, 44 seconds. Two functional scans were collected using a BOLD sequence with the following acquisition parameters: 72 axial slices, interleaved; phase encoding anterior-posterior; voxel size = 2 mm isotropic; matrix = 104 × 104; FOV = 208 mm; volumes = 388; TR = 800 ms; TE = 37 ms; and flip angle = 50°.

fMRI data processing was carried out using fMRI Expert Analysis Tool version 6.0, part of FMRIB's Software Library 5.0.7 (FSL v5.0.7, https://fsl.fmrib.ox.ac.uk/fsl/fslwiki; ref. 46). The following prestatistics processing was applied: motion correction using MCFLIRT (47), removal of nonbrain tissue using Brain Extraction Tool (48), spatial smoothing using a Gaussian kernel of 5 mm full width at half maximum, grand-mean intensity normalization of the entire 4-dimensional data set by a single multiplicative factor, and high-pass temporal filtering (Gaussian-weighted least-squares straight line fitting, with $\Sigma = 31.0$ seconds). In a 2-step registration process, each functional image was registered to that participant's T1-weighted structural image using FMRIB Linear Image Registration Tool, after which between-subject registration was accomplished by aligning each functional image to the MNI152 standard space template using the FMRIB Nonlinear Image Registration Tool. All images were visually inspected to ensure data quality (i.e., no excessive motion or artifacts) and ensure that proper nonbrain tissue masking and between-scan alignments were applied.

Statistics

Behavioral data statistical approach. Statistical analyses for behavioral data and extracted fMRI PEs were carried out using IBM SPSS Statistics version 24. All behavioral data were assessed for outliers and normal distribution before analysis. Means and SDs were computed for RT and response accuracy across all trials for each of the 2 experimental conditions (insulin and saline). Paired-sample *t* tests (2-tailed, $\alpha = 0.05$) were used to statistically compare within-subject differences among variables of interest between experimental conditions (insulin and saline) as reported in "Assessment of insulin sensitivity" and "Behavioral fMRI task results." Associations between 2 dichotomous variables were assessed using bivariate correlation models, and significant results are reported as resultant Pearson product moment correlation coefficients with an α level of 0.05.

fMRI statistical analysis. Time series statistical analysis was carried out using FMRIB's Improved Linear Model with local autocorrelation correction (49). Within each run, block onset times (0-back and 2-back blocks, alternating) were convolved with a single-γ hemodynamic response function to model BOLD signal activity associated with each behavioral condition. The 2-back to 0-back was the primary contrast of interest and served as input for all subsequent higher-level analyses.

Two statistical approaches were taken for higher-level analyses (50, 51). First, to visually assess BOLD signal activation on 2-back compared with 0-back trials for each experimental condition *separately* (insulin and saline), lower-level within-subject analyses were conducted to determine the difference in BOLD signal for the 2-back to 0-back contrast using a fixed-effects model, forcing the random-effects variance to 0 in FMRIB's Local Analysis of Mixed Effects - Option 1 (FLAME 1) (50). Subject-level *Z*-statistic images were thresholded using clusters determined by $Z > 2.3$ and a (corrected) cluster significance threshold of $P = 0.05$. To create a group-level map, 3D cope images of the 2-back to 0-back contrast served as input into a mixed-effects model using FLAME 1, resulting in a 1-sample group mean of task-related activation for 2-back to 0-back trials for insulin and saline conditions separately, with resulting *Z*-statistic maps thresholded using clusters determined by $Z > 2.3$ ($P < 0.01$) and a corrected cluster significance threshold of $P = 0.05$.

Second, to detect which regions demonstrated a statistically significant difference in BOLD signal *between* experimental conditions (insulin versus saline), a 2-step analysis was performed. First, subject-level repeated-measure analysis was performed to yield a single cope comparing BOLD signal during the contrast of interest (2-back to 0-back) between insulin and saline runs. Next, each within-subject difference cope was entered into a single-regression model to identify brain regions that consistently demonstrated a change in BOLD signal during the 2-back task between the insulin and saline conditions, such that the mean change in activation across all participants was significantly different from the null hypothesis of no change. Final *Z*-statistic maps were thresholded using clusters determined by $Z > 2.3$ ($P < 0.01$) and a corrected cluster significance threshold of $P < 0.05$. Final corrected clusters were used as ROIs for extracting

subject-level PEs per condition (insulin and saline) to use in additional statistical analyses. Because of the small sample size and thus limited statistical power of this study, covariates of interest were not included in the initial fMRI regression models but were analyzed post hoc within resulting significant ROIs.

Study approval. This study was conducted in accordance with the Declaration of Helsinki principles and approved by the Institutional Review Board of Partners Healthcare, Massachusetts General Hospital, Boston. All subjects provided written informed consent before inclusion in the study.

Author contributions

VJW is the lead and corresponding author on the manuscript and contributed significantly to data collection, analytic design, statistical analysis, results interpretation, and manuscript preparation. BAT assisted with data collection, biofluid processing, and manuscript revision. AMK contributed to study design, data collection, and manuscript revision. CDW assisted with data collection, participant recruitment, and scheduling. BCC significantly contributed to biofluid processing and manuscript revision. LE assisted with study design and manuscript revision. RSA significantly contributed to study design and conceptualization and manuscript revision. RZJ contributed to study design, data collection, results interpretation, and manuscript revision. SJR contributed to study design and conceptualization, data collection, results interpretation, and manuscript revision. DHS contributed to study design, results interpretation, and manuscript revision. SEA is the principal investigator on the project and led study conceptualization and design, results interpretation, and manuscript revision preparation and revision.

Acknowledgments

This work was funded by the NIH (5R21AG051958, 2016).

Address correspondence to: Victoria J. Williams, Alzheimer's Clinical and Translational Research Unit (ACTRU), Massachusetts General Hospital, Department of Neurology, 149 13th St., Charlestown, Massachusetts 02129, USA. Phone: 617.726.6215; Email: victoria.williams@mgh.harvard.edu.

AMK's present address is: Sage Therapeutics, Cambridge, Massachusetts, USA.

LE's present address is: Department of Pediatrics, Stanford Medicine, Stanford University, Palo Alto, California, USA.

1. [No authors listed]. National Diabetes Statistics Report, 2017. Centers for Disease Control Prevention. https://www.cdc.gov/diabetes/data/statistics-report/index.html. Update March 6, 2018. Accessed July 11, 2019.
2. Burns JM, Honea RA, Vidoni ED, Hutfles LJ, Brooks WM, Swerdlow RH. Insulin is differentially related to cognitive decline and atrophy in Alzheimer's disease and aging. *Biochim Biophys Acta*. 2012;1822(3):333–339.
3. Young SE, Mainous AG, Carnemolla M. Hyperinsulinemia and cognitive decline in a middle-aged cohort. *Diabetes Care*. 2006;29(12):2688–2693.
4. Willette AA, et al. Insulin resistance, brain atrophy, and cognitive performance in late middle-aged adults. *Diabetes Care*. 2013;36(2):443–449.
5. Ryu SY, Coutu JP, Rosas HD, Salat DH. Effects of insulin resistance on white matter microstructure in middle-aged and older adults. *Neurology*. 2014;82(21):1862–1870.
6. Willette AA, Modanlo N, Kapogiannis D, Alzheimer's Disease Neuroimaging Initiative. Insulin resistance predicts medial temporal hypermetabolism in mild cognitive impairment conversion to Alzheimer disease. *Diabetes*. 2015;64(6):1933–1940.
7. Hoscheidt SM, et al. Insulin resistance is associated with lower arterial blood flow and reduced cortical perfusion in cognitively asymptomatic middle-aged adults. *J Cereb Blood Flow Metab*. 2017;37(6):2249–2261.
8. Clarke DW, Boyd FT, Kappy MS, Raizada MK. Insulin binds to specific receptors and stimulates 2-deoxy-D-glucose uptake in cultured glial cells from rat brain. *J Biol Chem*. 1984;259(19):11672–11675.
9. Ghasemi R, Haeri A, Dargahi L, Mohamed Z, Ahmadiani A. Insulin in the brain: sources, localization and functions. *Mol Neurobiol*. 2013;47(1):145–171.
10. Heni M, Kullmann S, Preissl H, Fritsche A, Häring HU. Impaired insulin action in the human brain: causes and metabolic consequences. *Nat Rev Endocrinol*. 2015;11(12):701–711.
11. Boyd FT, Clarke DW, Muther TF, Raizada MK. Insulin receptors and insulin modulation of norepinephrine uptake in neuronal cultures from rat brain. *J Biol Chem*. 1985;260(29):15880–15884.
12. García-Cáceres C, et al. Astrocytic insulin signaling couples brain glucose uptake with nutrient availability. *Cell*. 2016;166(4):867–880.
13. De Felice FG, Lourenco MV, Ferreira ST. How does brain insulin resistance develop in Alzheimer's disease? *Alzheimers Dement*. 2014;10(1 Suppl):S26–S32.
14. de la Monte SM. Insulin resistance and Alzheimer's disease. *BMB Rep*. 2009;42(8):475–481.

15. Frölich L, et al. Brain insulin and insulin receptors in aging and sporadic Alzheimer's disease. *J Neural Transm (Vienna)*. 1998;105(4–5):423–438.
16. Talbot K, et al. Demonstrated brain insulin resistance in Alzheimer's disease patients is associated with IGF-1 resistance, IRS-1 dysregulation, and cognitive decline. *J Clin Invest*. 2012;122(4):1316–1338.
17. Correia SC, Santos RX, Perry G, Zhu X, Moreira PI, Smith MA. Insulin-resistant brain state: the culprit in sporadic Alzheimer's disease? *Ageing Res Rev*. 2011;10(2):264–273.
18. Dineley KT, Jahrling JB, Denner L. Insulin resistance in Alzheimer's disease. *Neurobiol Dis*. 2014;72(Pt A):92–103.
19. Benedict C, et al. Intranasal insulin improves memory in humans. *Psychoneuroendocrinology*. 2004;29(10):1326–1334.
20. Craft S, et al. Enhancement of memory in Alzheimer disease with insulin and somatostatin, but not glucose. *Arch Gen Psychiatry*. 1999;56(12):1135–1140.
21. Craft S, et al. Memory improvement following induced hyperinsulinemia in Alzheimer's disease. *Neurobiol Aging*. 1996;17(1):123–130.
22. Kern W, Peters A, Fruehwald-Schultes B, Deininger E, Born J, Fehm HL. Improving influence of insulin on cognitive functions in humans. *Neuroendocrinology*. 2001;74(4):270–280.
23. Craft S, et al. Insulin effects on glucose metabolism, memory, and plasma amyloid precursor protein in Alzheimer's disease differ according to apolipoprotein-E genotype. *Ann N Y Acad Sci*. 2000;903:222–228.
24. Benedict L, Nelson CA, Schunk E, Sullwold K, Seaquist ER. Effect of insulin on the brain activity obtained during visual and memory tasks in healthy human subjects. *Neuroendocrinology*. 2006;83(1):20–26.
25. Hasselbalch SG, et al. No effect of insulin on glucose blood-brain barrier transport and cerebral metabolism in humans. *Diabetes*. 1999;48(10):1915–1921.
26. Seaquist ER, et al. Insulin reduces the BOLD response but is without effect on the VEP during presentation of a visual task in humans. *J Cereb Blood Flow Metab*. 2007;27(1):154–160.
27. Tschritter O, et al. The cerebrocortical response to hyperinsulinemia is reduced in overweight humans: a magnetoencephalographic study. *Proc Natl Acad Sci U S A*. 2006;103(32):12103–12108.
28. Krulich L, Koenig JI, Conway S, McCann SM, Mayfield MA. Opioid kappa receptors and the secretion of prolactin (PRL) and growth hormone (GH) in the rat. II. GH and PRL release-inhibiting effects of the opioid kappa receptor agonists bremazocine and U-50,488. *Neuroendocrinology*. 1986;42(1):82–87.
29. Hirvonen J, et al. Effects of insulin on brain glucose metabolism in impaired glucose tolerance. *Diabetes*. 2011;60(2):443–447.
30. Rotte M, et al. Insulin affects the neuronal response in the medial temporal lobe in humans. *Neuroendocrinology*. 2005;81(1):49–55.
31. Grillo CA, Piroli GG, Hendry RM, Reagan LP. Insulin-stimulated translocation of GLUT4 to the plasma membrane in rat hippocampus is PI3-kinase dependent. *Brain Res*. 2009;1296:35–45.
32. DeFronzo RA, Tobin JD, Andres R. Glucose clamp technique: a method for quantifying insulin secretion and resistance. *Am J Physiol*. 1979;237(3):E214–E223.
33. Vannucci SJ. Developmental expression of GLUT1 and GLUT3 glucose transporters in rat brain. *J Neurochem*. 1994;62(1):240–246.
34. Morgello S, Uson RR, Schwartz EJ, Haber RS. The human blood-brain barrier glucose transporter (GLUT1) is a glucose transporter of gray matter astrocytes. *Glia*. 1995;14(1):43–54.
35. Simpson IA, Carruthers A, Vannucci SJ. Supply and demand in cerebral energy metabolism: the role of nutrient transporters. *J Cereb Blood Flow Metab*. 2007;27(11):1766–1791.
36. Gould GW, Thomas HM, Jess TJ, Bell GI. Expression of human glucose transporters in Xenopus oocytes: kinetic characterization and substrate specificities of the erythrocyte, liver, and brain isoforms. *Biochemistry*. 1991;30(21):5139–5145.
37. Bingham EM, et al. The role of insulin in human brain glucose metabolism: an 18fluoro-deoxyglucose positron emission tomography study. *Diabetes*. 2002;51(12):3384–3390.
38. Emmanuel Y, Cochlin LE, Tyler DJ, de Jager CA, Smith AD, Clarke K. Human hippocampal energy metabolism is impaired during cognitive activity in a lipid infusion model of insulin resistance. *Brain Behav*. 2013;3(2):134–144.
39. Morris JK, et al. Cognitively impaired elderly exhibit insulin resistance and no memory improvement with infused insulin. *Neurobiol Aging*. 2016;39:19–24.
40. Craft S, et al. Effects of regular and long-acting insulin on cognition and Alzheimer's disease biomarkers: a pilot clinical trial. *J Alzheimers Dis*. 2017;57(4):1325–1334.
41. Craft S, et al. Intranasal insulin therapy for Alzheimer disease and amnestic mild cognitive impairment: a pilot clinical trial. *Arch Neurol*. 2012;69(1):29–38.
42. Kullmann S, et al. Intranasal insulin enhances brain functional connectivity mediating the relationship between adiposity and subjective feeling of hunger. *Sci Rep*. 2017;7(1):1627.
43. Gonzales MM, Tarumi T, Miles SC, Tanaka H, Shah F, Haley AP. Insulin sensitivity as a mediator of the relationship between BMI and working memory-related brain activation. *Obesity (Silver Spring)*. 2010;18(11):2131–2137.
44. Kullmann S, et al. The obese brain: association of body mass index and insulin sensitivity with resting state network functional connectivity. *Hum Brain Mapp*. 2012;33(5):1052–1061.
45. Gutch M, Kumar S, Razi SM, Gupta KK, Gupta A. Assessment of insulin sensitivity/resistance. *Indian J Endocrinol Metab*. 2015;19(1):160–164.
46. Jenkinson M, Beckmann CF, Behrens TE, Woolrich MW, Smith SM. FSL. *Neuroimage*. 2012;62(2):782–790.
47. Jenkinson M, Bannister P, Brady M, Smith S. Improved optimization for the robust and accurate linear registration and motion correction of brain images. *Neuroimage*. 2002;17(2):825–841.
48. Smith SM. Fast robust automated brain extraction. *Hum Brain Mapp*. 2002;17(3):143–155.
49. Woolrich MW, Ripley BD, Brady M, Smith SM. Temporal autocorrelation in univariate linear modeling of FMRI data. *Neuroimage*. 2001;14(6):1370–1386.
50. Woolrich MW, Behrens TE, Beckmann CF, Jenkinson M, Smith SM. Multilevel linear modelling for FMRI group analysis using Bayesian inference. *Neuroimage*. 2004;21(4):1732–1747.
51. Woolrich MW, et al. Bayesian analysis of neuroimaging data in FSL. *Neuroimage*. 2009;45(suppl_1):S173–S186.